RAPID COMMUNICATION

Magnetoresistivity and filamentary superconductivity in nickel-doped $BaFe_2As_2$*

Wei Zhang(张威)[1,2], Yao-Min Dai(戴耀民)[2], Bing Xu(许兵)[2], Run Yang(杨润)[2], Jin-Yun Liu(刘金云)[2], Qiang-Tao Sui(随强涛)[2], Hui-Qian Luo(罗会仟)[2], Rui Zhang(张睿)[2], Xing-Ye Lu(鲁兴业)[2], Hao Yang(杨浩)[3,†], and Xiang-Gang Qiu(邱祥冈)[2,‡]

[1] *College of Physics, Optoelectronics and Energy and Collaborative Innovation Center of Suzhou Nano Science and Technology, Soochow University, Suzhou* 215006, *China*

[2] *Beijing National Laboratory for Condensed Matter Physics, Institute of Physics, Chinese Academy of Sciences, Beijing* 100190, *China*

[3] *College of Science, Nanjing University of Aeronautics and Astronautics, Nanjing* 211106, *China*

(Received 7 January 2016; revised manuscript received 28 January 2016; published online 20 February 2016)

We present magnetotransport studies on a series of $BaFe_{2-x}Ni_xAs_2$ ($0.03 \leq x \leq 0.10$) single crystals. In the underdoped ($x = 0.03$) non-superconducting sample, the temperature-dependent resistivity exhibits a peak at 22 K, which is associated with the onset of filamentary superconductivity (FLSC). FLSC is suppressed by an external magnetic field in a manner similar to the suppression of bulk superconductivity in an optimally-doped ($x = 0.10$) compound, suggesting the same possible origin as the bulk superconductivity. Our magnetoresistivity measurements reveal that FLSC persists up to the optimal doping and disappears in the overdoped regime where the long-range antiferromagnetic order is completely suppressed, pointing to a close relation between FLSC and the magnetic order.

Keywords: iron-based pnictide, magnetoresistivity, filamentary superconductivity

PACS: 74.25.DW, 74.25.F–, 74.70.Xa, 74.81.–g **DOI:** 10.1088/1674-1056/25/4/047401

1. Introduction

The discovery of unconventional superconductivity in iron pnictides[1] has aroused a tremendous amount of research into this class of materials in an effort to understand the mechanism of high-T_c superconductivity, as well as to explore materials with higher T_c. The parent compounds of these iron-based superconductors (FeSCs) are poor Pauli-paramagnetic metals in their high-temperature phase, and undergo structural and antiferromagnetic (AFM) phase transitions upon cooling down to low temperature.[2–4] Superconductivity emerges with the suppression of the AFM order via chemical substitution[5–7] or the application of pressure.[8–11] Since optimal superconductivity is accompanied by the disappearance of the AFM phase, AFM spin fluctuations have been proposed to mediate the electronic pairing in FeSCs.[12] On the other hand, previous spectroscopic studies have also revealed strong competition between the AFM order and superconductivity in the Ba122 system.[13,14] Therefore, the relation between magnetism and superconductivity is still a matter of debate in FeSCs.

In this article, we report our results of magnetotransport measurements on $BaFe_{2-x}Ni_xAs_2$ single crystals with different Ni concentration. An abrupt drop of the resistivity at ~ 22 K in underdoped $x = 0.03$ has been observed in the temperature-dependent resistivity as evidence for the onset of filamentary superconductivity (FLSC). An external magnetic field suppresses FLSC in a manner similar to the suppression of the bulk T_c in an optimally-doped ($x = 0.10$) sample, suggesting a possible connection between FLSC and bulk SC. In addition, FLSC is robust and exhibits little doping dependence in the underdoped regime, but vanishes abruptly in the overdoped region where long-range AFM order is absent. These results indicate that the emergence of FLSC is intimately related to the magnetic order in FeSCs.

2. Experiments

High-quality single crystals of $BaFe_{2-x}Ni_xAs_2$ with a series of Ni doping were grown using a self-flux method.[15] Typical dimensions of single crystals for measurements are approximately 1 mm × 0.25 mm × 0.05 mm. In-plane resistivity was measured as a function of temperature in a physical property measurements system (PPMS-9, Quantum Design) using a standard four-electrode method. The current used for measurements is parallel to the basel plane and $I = 1$ mA.

3. Results and discussion

Figure 1 shows the temperature dependence of normalized resistivity $\rho(T)/\rho(300\ \mathrm{K})$ for $x = 0.03$ underdoped and

*Project supported by the National Basic Research Program of China (Grant Nos. 2012CB821400, 2012CB921302, and 2015CB921303) and the National Natural Science Foundation of China (Grant Nos. 11274237, 91121004, 51228201, 11004238, and 11374011).

†Corresponding author. E-mail: yanghao@nuaa.edu.cn

‡Corresponding author. E-mail: xgqiu@iphy.ac.cn

© 2016 Chinese Physical Society and IOP Publishing Ltd

$x = 0.10$ optimally doped $BaFe_{2-x}Ni_xAs_2$ samples. For $x = 0.10$, the curve is characterized by a steep superconducting transition at $T_c = 20.3$ K. The $x = 0.03$ sample features a metallic behavior followed by an upturn resistivity at the spin-density-wave (SDW) transition temperature $T_N = 109$ K, corresponding to a sharp dip in the derivative of the resistivity $d\rho/dT$ as a function of temperature. Meanwhile, as shown in the upper inset in Fig. 1, an abrupt drop of resistivity can be clearly identified at low temperature $T_{fl} \approx 22$ K for the $x = 0.03$ sample. Our recent studies on $CaFe_2As_2$[16] and $BaFe_{2-x}Co_xAs_2$[17] has demonstrated that this step in the resistivity is due to the presence of weakly pinned superconducting filaments. Furthermore, we have also provided evidence that filamentary superconductivity nucleated at antiphase domain walls in antiferromagnetic $CaFe_2As_2$. Therefore, we define the temperature of this step in resistivity as the onset of FLSC (T_{fl}), similar to the high-T_c cuprates[18,19] and heavy fermions superconductors.[20,21]

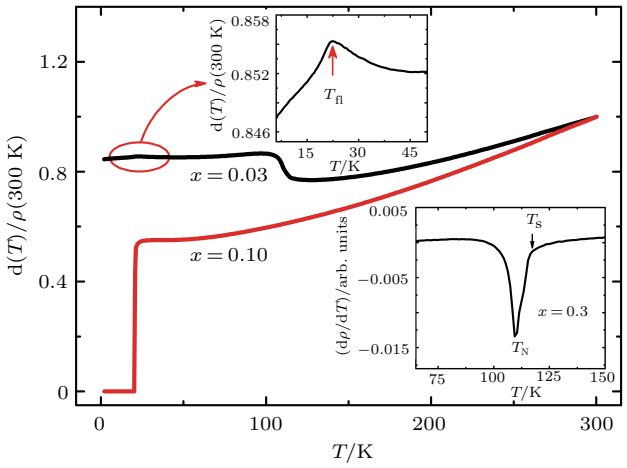


Fig. 1. (color online) The temperature-dependent normalized resistivity $\rho(T)/\rho(300\ \mathrm{K})$ curves for $BaFe_{2-x}Ni_xAs_2$ single crystals with $x = 0.03$ and $x = 0.10$. Top inset: the enlarged view of $\rho(T)/\rho(300\ \mathrm{K})$ curve for underdoped $x = 0.03$ sample; Bottom inset: the derivative curve $d\rho/dT$ for $x = 0.03$ sample.

The top panel of Fig. 2 shows $\rho(T)$ curves from 2 K to 110 K at different magnetic fields for underdoped $BaFe_{2-x}Ni_xAs_2$ ($x = 0.03$). While no magnetoresistance is observed above the magnetic transition temperature T_N, a peak feature related to FLSC is observed at temperature T_{fl} in all curves. It is noticed that T_{fl} decreases with increasing magnetic fields. The H–T phase diagram obtained from the field dependence of T_{fl} for the $x = 0.03$ sample and the field dependence of bulk T_c for the $x = 0.10$ sample are shown in the bottom panel of Fig. 2. A striking similarity of the suppression by external magnetic field between T_{fl} and T_c is found through the comparison of these H–T phase diagrams, which suggests a close connection between FLSC and bulk SC and rules out the possible contribution of an impurity phase to this phenomena.

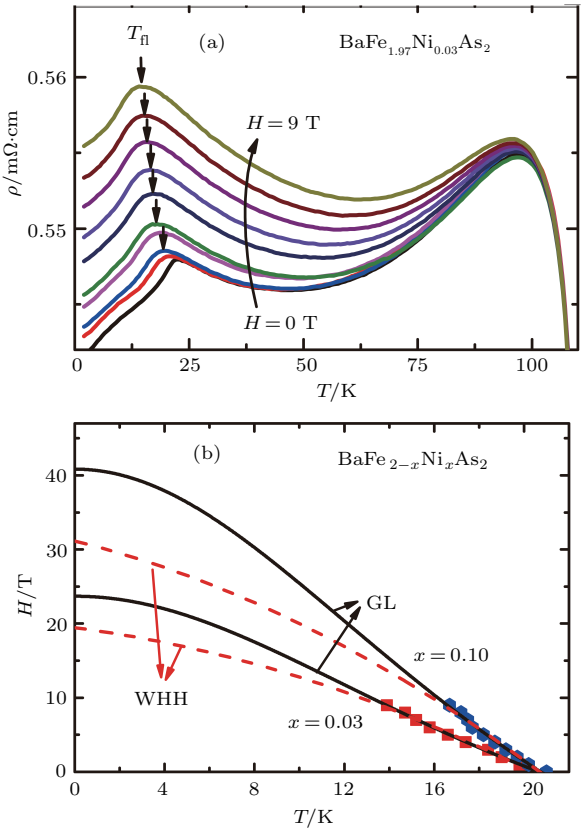


Fig. 2. (color online) (a) Temperature-dependent reduced resistivity $\rho(T)/\rho(300\ \mathrm{K})$ curves for $BaFe_{1.97}Ni_{0.03}As_2$ single crystal with different applied magnetic fields ($H = 1$ T–9 T). (b) H–T phase diagrams of $BaFe_{2-x}Ni_xAs_2$ single crystal ($x = 0.03$ and $x = 0.10$). The black solid lines are fits of the data by using the GL expression, the red dotted lines are fits with the Werthemer–Helfand–Hohenberg (WHH) model.

In addition, the upper critical fields in these two samples are also fitted by the Ginzburg–Landau (GL) model and the Werthamer–Helfand–Hohenberg (WHH) model. As shown in the bottom panel of Fig. 2, the solid curve is a fit with GL expression,

$$H_{c_2}(T) = \frac{H_{c_2}(0)\left[1-\left(T/T_c\right)^2\right]}{\left[1+\left(T/T_c\right)^2\right]},$$

which gives $H_{c_2}(0) = 23.7$ T and $T_c = 20.6$ K for the underdoped $x = 0.03$ sample, and $H_{c_2}(0) = 40.8$ T and $T_c = 20.7$ K for the optimally-doped $x = 0.10$ sample. The dashed curve is a fit with the WHH relation, $H_{c_2}(0) = -0.7T_c(dH_{c_2}/dT_c)$, which gives a slope of -1.34 T/K and $H_{c_2}(0) = 19.4$ T with $T_c = 20.6$ K for the $x = 0.03$ sample, and a slope of -2.14 T/K and $H_{c_2}(0) = 31.1$ T with $T_c = 20.7$ K for the $x = 0.10$ sample. The value of $H_{c_2}(0)$ obtained from WHH is lower than GL, which is similar to that reported in other 122-type iron pnictide superconductors.[22] Meanwhile, it is noted that recently Wang *et al.* reported that the H_{c2}^c of $x = 0.10$ sample with high field data can be described by a two-band model and it gave a higher $H_{c2} = 47.5$ T.[23]

While we observed an obvious drop of resistivity in $\rho(T)$ curves for the $x = 0.03$ sample, some studies showed that the

step in the low-temperature resistivity is not always observed in 122-type parent compound in iron pnictide superconductors. For example, Xiao *et al.* reported that this step was observed only for small and thin single crystals in undoped $BaFe_2As_2$.[17] Tanatar *et al.* studied different samples of parent compounds $CaFe_2As_2$ and $BaFe_2As_2$, and found that two samples showed the partial superconducting transition in three undoped $CaFe_2As_2$, and even only two samples showed the partial superconducting transition in five different $BaFe_2As_2$ samples.[24] For this reason, we performed magnetoresistivity measurements, which is believed to be more sensitive to the small decrease in resistivity due to filamentary superconductivity.

Figure 3 shows the temperature dependence of magnetoresistivity $\Delta\rho/\rho(0) = [\rho(9\,\mathrm{T}) - \rho(0\,\mathrm{T})]/\rho(0\,\mathrm{T})$ for different Ni concentrations. As the temperature decreases, the magnetoresistivity $\Delta\rho/\rho(0)$ for the underdoped $x = 0.03$ sample increases very gently at first, but then an abrupt increase occurs close to 22 K, which is exactly the FLSC onset temperature T_{fl} in the zero-field $\rho(T)$ curve. Therefore, we attribute this abrupt change in magnetoresistivity to the occurrence of filamentary superconductivity and identify the temperature as T_{fl}. We also performed magnetoresistivity measurements on several other pieces of crystal of underdoped $x = 0.03$ samples and confirmed that the abrupt change in magnetoresistivity always exists at a temperature T_{fl} even in some samples where the step in $\rho(T)$ curve has not been detected. Furthermore, the abrupt change in magnetoresistivity is observed in other Ni-doping $BaFe_{2-x}Ni_xAs_2$ single crystals in Fig. 3.

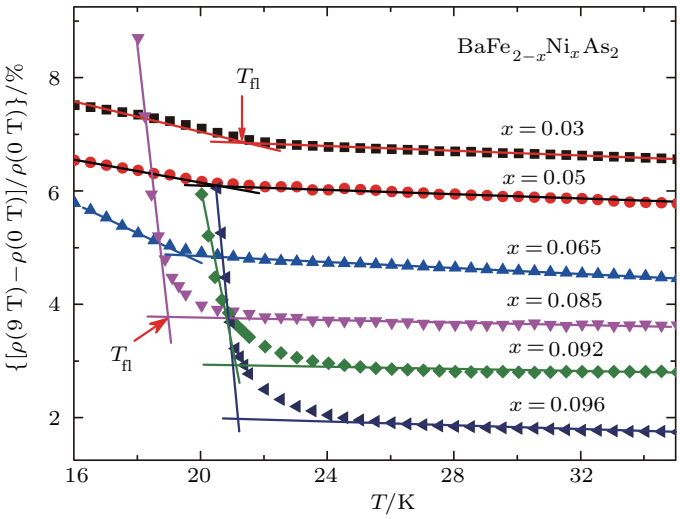


Fig. 3. (color online) (a) Temperature-dependent magnetoresistivity $[\rho(9\,\mathrm{T}) - \rho(0\,\mathrm{T})]/\rho(0\,\mathrm{T})$ curves for $BaFe_{2-x}Ni_xAs_2$ single crystals with $x = 0.03, 0.05, 0.065, 0.085, 0.092$, and 0.096. Data were offset vertically to separate the overlapped curves between different doping.

In Fig. 4, we make a comprehensive plot of the phase diagram of the doping dependence of structural transition temperature T_s, magnetic transition temperature T_N, superconducting transition temperature T_c, and FLSC transition temperature T_{fl}. The defination of T_s, T_N, and T_c is shown in Fig. 1. From the phase diagram we find that the parent compound $BaFe_2As_2$ exhibits simultaneous structural and magnetic phase transitions at ~ 140 K, from high-temperature tetragonal paramagnetic to low-temperature orthorhombic antiferromagnetic phase. With increasing Ni doping, the structural and magnetic transitions separate from each other with T_N slightly lower than T_s. The antiferromagnetic order is suppressed by replacing Fe by Ni in $BaFe_2As_2$. Superconductivity emerges at $x \approx 0.05$ and reaches a maximum at $x = 0.10$ where long-range AFM order vanishes. Most importantly, we find that T_{fl} is less doping dependent compared with the bulk superconductivity T_c and it exists in underdoped samples and persists up to the edge of the optimally-doped $x = 0.10$ sample, where the AFM order vanishes. This suggests a close relationship between FLSC and AFM order.

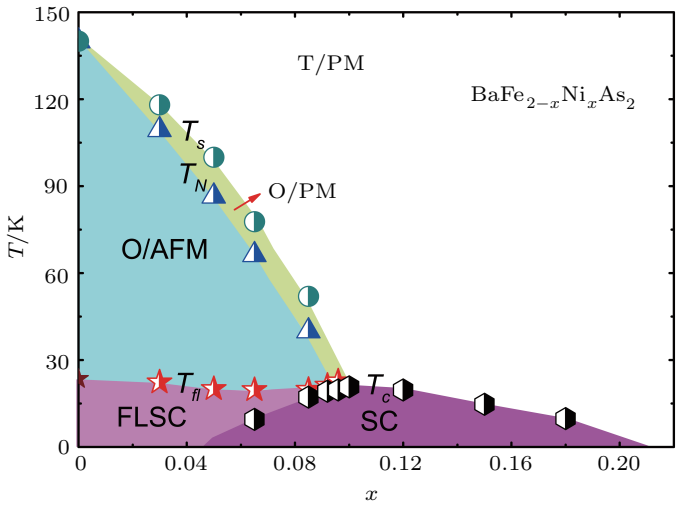


Fig. 4. (color online) Doping-x dependence of T_s, T_N, T_c, and T_{fl} phase diagram. T_{fl} in parent compound $BaFe_2As_2$ is obtained from Ref. [17].

However, some recent experimental results revealed that SC and AFM order parameters are spatially modulated on a microscopic scale in iron pnictides.[24–26] For example, many studies showed the evidence for the existence of the structural domain like twin boundary and antiphase domain wall in the iron pictides.[24,26] Meanwhile, a recent SQUID microscopy study in underdoped $Ba(Fe_{1-x}Co_x)_2As_2$ showed an enhanced superfluid density on twin boundaries[25] and ^{75}As nuclear magnetic resonance (NMR) measurements in antiferromagnetic $CaFe_2As_2$ suggests the presence of FLSC nucleated at the AFM domain walls.[16] All these results indicate that AFM order is vital to the emergence of SC in iron pnictides.

In combination with our previous studies in $CaFe_2As_2$ and $Ba(Fe_{1-x}Co_x)_2As_2$,[16,17] we find that FLSC exists in electron-doped 122-type iron-based superconductors and it has a close connection with AFM order. Besides, Chu *et al.* also revealed an obvious FLSC with a high $T_c = 49$ K in single

crystalline $CaFe_2As_2$ via electron-doping by partial replacement of Ca by rare-earth.[27,28] Thus our results suggest that the FLSC may be a common feature in the AFM phase of iron pnictides due to strong coupling between AFM and superconductivity, further exploration is needed to verify it.

4. Conclusion

In conclusion, magnetotransport measurements have been carried out on a series of Ni doping $BaFe_2As_2$ single crystals. A similar suppression of FLSC T_{fl} and bulk SC T_c by external magnetic field is depicted in the H–T phase diagram. The doping-temperature phase diagram reveals the following results: (i) FLSC is less doping-dependent compared with bulk SC; (ii) FLSC coexists with AFM order and vanishes in the edge of optimal doping where long-range AFM order is absent. Based on our results, we conclude that FLSC is closely linked with magnetic order and the bulk SC in iron pnictides.

References

[1] Kamihara Y, Watanabe T, Hirano M and Hosono H 2008 *J. Am. Chem. Soc.* **130** 3296

[2] Ni N, Nandi S, Kreyssig A, Goldman A I, Mun E D, Bud'ko S L and Canfield P C 2008 *Phys. Rev. B* **78** 014523

[3] Huang Q, Qiu Y, Bao W, Green M A, Lynn J W, Gasparovic Y C, Wu T, Wu G, and Chen X H 2008 *Phys. Rev. Lett.* **101** 257003

[4] Rotter M, Tegel M, Johrendt D, Schellenberg I, Hermes W and Pöttgen R 2008 *Phys. Rev. B* **78** 020503

[5] Rotter M, Tegel M and Johrendt D 2008 *Phys. Rev. Lett.* **101** 107006

[6] Ni N, Thaler A, Yan J Q, Kracher A, Colombier E, Bud'ko S L, Canfield P C and Hannahs S T 2010 *Phys. Rev. B* **82** 024519

[7] Jiang S, Xing H, Xuan G, Wang C, Ren Z, Feng C, Dai J, Xu Z and Gao G 2009 *J. Phys.: Condens. Matter* **21** 382203

[8] Torikachvili M S, Bud'ko S L, Ni N, and Canfield P C 2008 *Phys. Rev. Lett.* **101** 057006

[9] Park T, Park E, Lee H, Klimczuk T, Bauer E D, Ronning F and Thompson J D 2008 *J. Phys.: Condens. Matter* **20** 322204

[10] Alireza P L, Ko Y T C, Gillett J, Petrone C M, Cole J M, Lonzarich G G, and Sebastian S E 2009 *J. Phys.: Condens. Matter* **21** 012208

[11] Kitagawa K, Katayama N, Gotou H, Yagi T, Ohgushi K, Matsumoto T, Uwatoko Y and Takigawa 2009 *Phys. Rev. Lett.* **103** 257002

[12] Mazin I I, Singh D J, Johannes M D and Takigawa M 2008 *Phys. Rev. Lett.* **101** 057003

[13] Chia E E M, Talbayev D, Zhu J X, Yuan H Q, Park T, Thompson J D, Panagopoulos C, Chen G F, Luo J L, Wang N L and Taylor A J 2010 *Phys. Rev. Lett.* **104** 027003

[14] Dai Y M, Xu B, Shen B, Wen H H, Hu J P, Qiu X G and Lobo R O S M 2012 *Phys. Rev. B* **86** 100501

[15] Chen Y, Lu X, Wang M, Luo H and Li S 2011 *Supercond. Sci. Technol.* **24** 065004

[16] Xiao H, Hu T, Dioguardi A P, Roberts-Warren N, Shockley A C, Crocker J, Nisson D M, Viskadourakis Z, Tee X Y, Radulov I, Almasan C C, Curro N J and Panagopoulos C 2012 *Phys. Rev. B* **85** 024530

[17] Xiao H, Hu T, He S K, Shen B, Zhang W J, Xu B, He K F, Han J, Singh Y P, Wen H H, Qiu X G, Panagopoulos C and Almasan C C 2012 *Phys. Rev. B* **86** 064521

[18] Gomes K K, Pasupathy A N, Pushp A, Ono S, Ando Y and Yazdani A 2007 *Nature* **447** 569

[19] Li Q, Hücker M, Gu G D, Tsvelik A M and Tranquada J M 2007 *Phys. Rev. Lett.* **99** 067001

[20] Bianchi A, Movshovich R, Jaime M, Thompson J D, Pagliuso and Sarrao J L 2001 *Phys. Rev. B* **64** 220504

[21] Chen Y, Jiang W B, Guo C Y, Yuan H Q, Fisk Z, Thompson J D and Lu X 2015 *Phys. Rev. Lett.* **114** 146403

[22] Kumar N, Nagalakshmi R, Kulkarni R, Paulose P L, Nigam A K, Dhar S K and Thamizhavel A 2009 *Phys. Rev. B* **79** 012504

[23] Wang Z S, Xie T, Kampert E, Förster T, Lu X Y, Zhang R, Gong D L, Li S L, Herrmannsdörfer T, Wosnitza J and Luo H Q 2015 *Phys. Rev. B* **92** 174509

[24] Tanatar M A, Kreyssig A, Nandi, Ni N, Bud'ko S L, Canfield P C, Goldman A I and Prozorov 2009 *Phys. Rev. B* **79** 180508

[25] Kalisky B, Kirtley J R, Analytis J G, Chu J W, Vailionis A, Fisher I R and Moler K A 2010 *Phys. Rev. B* **81** 184513

[26] Li G, He X, Zhang J, Jin R, Sefat A S, McGuire M A, Mandrus D G, Sales B C and Plummer E W 2012 *Phys. Rev. B* **86** 060512

[27] Lv B, Deng L Z, Gooch M, Wei F Y, Sun Y Y, Meen J K, Xue Y Y, Lorenz B and Chu C W 2011 *Proc. Natl. Acad. Sci* **108** 15705

[28] Gofryk K, Pan M H, Cantoni C, Saparov B, Mitchell J and Sefat S 2014 *Phys. Rev. Lett.* **112** 047005